

A FLEXIBLE “ALE” FINITE ELEMENT PROCEDURE FOR THE ANALYSIS OF FLUID-STRUCTURE APPLICATIONS

Paulo R. M. Lyra

Mechanical Engineering Department, Federal University of Pernambuco, Recife/PE, Brasil, prmlyra@demec.ufpe.br

Alessandro R. E. Antunes

Mechanical Engineering Department, Federal University of Pernambuco, Recife/PE, Brasil, aantunes@demec.ufpe.br

Ramiro B. Willmersdorf

Mechanical Engineering Department, Federal University of Pernambuco, Recife/PE, Brasil, rbw@demec.ufpe.br

Abstract. *In this paper a flexible finite element computational tool developed to investigate fluid-structure interaction applications in two dimensions is briefly described. We consider problems which can be modelled as a viscous incompressible fluid flow and a rigid body-spring system interacting nonlinearly with each other. The coupling is dealt using an interface approach, in which each physics involved is solved with different schemes and the required information are passed through the interface of both system. This approach is, at least in principle, very flexible and computationally efficient as the best available scheme can be adopted to solve each physics. Here, a stabilized FEM considering the “ALE” (Arbitrary Lagrangian-Eulerian) formulation with Crank-Nicholson time-integration is employed for the fluid-dynamics analysis, and the Newmark Method is used for the structural analysis. Several important tools were incorporated into our system including different possibilities for: the mesh movement algorithm, the computational domain decomposition into regions with and without mesh deformation, and the remeshing strategy (either global or local) to keep the necessary mesh quality. As an application we present a preliminary study of the suppression (or at least the reduction) of the vortex induced vibrations (VIV) on a solid circular cylinder using periodic “acoustic” excitation.*

Keywords. *Fluid-structure interaction, vortex induced vibrations (VIV), finite element method (FEM), arbitrary Lagrangian-Eulerian (ALE) formulation, suppression of structural vibration*

1. Introduction

Several practical structures, in different engineering fields, are subjected to vibration as a result of flow induced phenomena. Such behavior can compromise the integrity of the structure or make uncomfortable for human use. The analysis of these problems involve the study of a coupled fluid-structure interaction model and can be done using computational modeling. The numerical simulation of such applications is most commonly performed using an interface approach and involves the modification of the computational domain as the geometry under consideration is moving with time. In order to avoid updating the computational discretization too frequently, an arbitrary Lagrangian Eulerian (ALE) formulation (Childs, 1999; Nomura and Hughes, 1992) is normally adopted together with a mesh movement algorithm. In such approach, generally, the reference frame at the moving interface between the structure and the fluid has a Lagrangian description and apart from that has a mixed Lagrangian and Eulerian description to accommodate the arbitrary movement of the frame of reference.

In this paper we briefly describe the finite element procedure developed to simulate the two dimensional fluid-structure interaction of a rigid circular cylinder, supported by elastic springs, immerse in an incompressible viscous fluid flow (Antunes et al., 2002, Lyra and Antunes, 2002 and Antunes, 2002). The analysis of such model application gives insight on many problems of industrial interest, for instance the study of “VIV” (Vortex Induced Vibrations) (Blevins, 1986) on offshore platform legs. The adopted procedure uses a stabilized Petrov-Galerkin/Generalized Least Squares “ALE” (Arbitrary Lagrangian-Eulerian) finite element formulation with Crank-Nicholson time-integration for the fluid-dynamics analysis (Sampaio et al., 1993). This scheme represents an SUPG-like algorithm (Streamline Upwind Petrov-Galerkin (Brooks and Hughes, 1982)) with the optimal upwind parameter implicitly determined through the formulation and a timescale analysis. For the structural analysis it uses a simple lumped model with three degrees-of-freedom and the Newmark Method (Hughes, 1987). The fluid-structural coupling is solved through interfacing and implemented in a segregated approach, using an algorithm to control errors due to the existing time delay between the fluid and structural analysis (Blom and Leyland, 1998). Several alternatives for the subdivision of domain into subdomains, where the different descriptions (Eulerian, Lagrangian or ALE) are adopted, were incorporated in our computational system. Different types of mesh movement and mesh smoothing were implemented in order to reduce the distortion of the computational meshes over the fluid domain. The capabilities of automatically generating and adapting the mesh (using local or global remeshing) (Carvalho, 2001) were also incorporated into the computational system, allowing the study of problems with large displacements. All these features will be briefly described. Further details and the results to many applications dealing with different levels of difficulty and interaction between fluid and structure were analyzed to validate the computational system developed and can be seen in Antunes et al. (2002), Lyra and Antunes (2002) and Antunes (2002). The obtained results are in good agreement with the experimental, theoretical and numerical data available in the literature. A preliminary numerical study on the suppression of the vortex-induced vibration of a circular cylinder by “acoustic” excitation is presented. The results shows the influence of the “acoustic” excitation frequency on the vortex shedding frequency and so on the amplitude of the structural vibration. Finally, we draw the most important conclusions and some on going and future extension of this research.

2. Numerical Formulation

Most fluid structure interaction problems where there is a strong coupling between the displacement of the structure and the flow field are characterized by large displacements of some of the boundaries of the domain. The regions close to these moving boundaries are more naturally discretized with a Lagrangean approach. The fluid regions away from the moving boundaries, however, are more naturally treated with a conventional Eulerian formulation, with a fixed reference frame. We use an Arbitrary Lagrangean Eulerian framework to combine these two approaches in a single numerical technique. The differential equations that described the dynamics of the fluid and the structure therefore must be written in this framework.

2.1. Standard Eulerian Formulation

The flow of incompressible fluids can be described by a specialization of the general Navier-Stokes Equations, where we will also consider that the viscosity is constant and that the fluid is Newtonian. Unless otherwise noted, in the following we will use indicial notation with the summation convention. Within an Eulerian framework, i.e., using a fixed frame of reference and fixed control volumes, the Navier-Stokes equations in non-conservative form reduce to:

$$\rho \frac{\partial u_i}{\partial t} + \rho u_j \frac{\partial u_i}{\partial x_j} = \frac{\partial \tau_{ij}}{\partial x_j} + b_i \quad (1)$$

In the above equation, $i = 1, 2$, x_i are the spatial coordinates, t is the time variable, ρ is the density of the fluid, u_i are the components of the velocity of the fluid, b_i are the external body forces, and τ_{ij} is the stress tensor. Equation (1) is subjected to the incompressibility restriction

$$\frac{\partial u_i}{\partial x_i} = 0; \quad (2)$$

and the stress tensor is given by

$$\tau_{ij} = -p\delta_{ij} + \mu \left(\frac{\partial u_i}{\partial x_j} + \frac{\partial u_j}{\partial x_i} \right) \quad (3)$$

where μ is the dynamic viscosity, p is the pressure and δ_{ij} is Kroenecker's delta. Equations (1), (2) and (3) are written for a fixed geometric domain Ω_f and for a time interval I . For a well posed problem, it is also necessary to impose to the above set of equations boundary conditions on Γ , the boundary of the domain Ω_f , and initial conditions on Ω_f . The boundary conditions are known velocities \bar{u} on Γ_u and known surface tractions \bar{t} on Γ_t , with $\Gamma = \Gamma_u \cup \Gamma_t$ and $\Gamma_u \cap \Gamma_t = 0$. The boundary conditions associated to the mass balance are given in terms of known pressure \bar{p} on Γ_p and known mass flux \bar{G} on Γ_G , with $\Gamma = \Gamma_p \cup \Gamma_G$ and $\Gamma_p \cap \Gamma_G = 0$. Here, $G = \rho u_i n_i$ with n_i being the outward pointing unit normal vector to Γ . The initial conditions are known velocities on Ω_f in the initial time of the analysis.

2.2. ALE Formulation

To develop a finite element discretization applicable to deformable domains, we use an ALE formulation, as proposed in Hughes et al (1981). We define three domains: the spatial domain Ω_y which is the physical space defined by the material particles at time t ; the referential domain Ω_x , which is a fixed domain whose image at time t , subjected to a transformation $\hat{\phi}$, is the spatial domain; and the material domain Ω_z , which is the domain occupied at the time $t=0$ by the material particles that occupy the spatial domain at time t . If we define the transformation from the material domain to the spatial domain as ϕ , i.e., $\phi: \Omega_z \rightarrow \Omega_y$, then the transformation from the material domain to the referential domain is given by $\psi: \Omega_z \rightarrow \Omega_x$, where $\psi = \hat{\phi}^{-1} \circ \phi$ (\circ is the functional composition operator). Now let us consider that z_i and x_i represent particles in Ω_z and Ω_x whose image at time t is y_i in Ω_y . Therefore, considering the transformation ϕ , we can write that:

$$u_i = y_i - z_i, \quad \dot{u}_i = \dot{y}_i \quad \text{and} \quad y_{i,j} = \frac{\partial y_i}{\partial z_j}, \quad (4)$$

where u_i is the displacement, \dot{u}_i is the velocity and $y_{i,j}$ is the deformation gradient. In a similar manner, considering the transformation $\hat{\phi}$, we can write:

$$\hat{u}_i = y_i - x_i, \quad \hat{u}'_i = y'_i \quad \text{and} \quad y_{ij} = \frac{\partial y_i}{\partial x_j}, \quad (5)$$

where \hat{u}_i is the displacement, \hat{u}'_i is the velocity and y_{ij} is the deformation gradient. Finally, considering the transformation ψ , we can write:

$$w_i = x_i - z_i, \quad \dot{w}_i = \dot{x}_i \quad \text{and} \quad x_{i,j} = \frac{\partial x_i}{\partial y_j}, \quad (6)$$

where w_i is the displacement, \dot{w}_i is the velocity and $y_{i,j}$ is the deformation gradient. Equations (4) to (6) are the kinematic relationships for the different descriptions of a continuum.

With the above mappings, we can write (Antunes, 2002) that:

$$c_i = \dot{u}_i - \hat{u}'_i = \frac{\partial y_i}{\partial x_j} \frac{\partial x_j}{\partial t} \quad (7)$$

where c_i is defined as the convective velocity. If f is a scalar function of the flow field, the material derivative of this function is given by (Childs, 1999):

$$\frac{Df}{Dt} = \frac{\partial f}{\partial t} + \frac{\partial f}{\partial x} F^{-1} c \quad (8)$$

where $F_{ij} = \frac{\partial y_i}{\partial x_j}$ is the deformation gradient between the reference and the spatial domain, and c_i is the convective velocity defined in Eq. (7). In this work, we used a single step Crank-Nicholson scheme for the time integration, therefore throughout the duration of each and every time step, the referential and spatial domains are coincident. The deformation gradient between these two domains is the identity transformation, so Eq. (8) reduces to:

$$\frac{Df}{Dt} = \frac{\partial f}{\partial t} + \frac{\partial f}{\partial x} c \quad (9)$$

It is well worth noting that if $\hat{u}'_i = 0$ in Eq. (7) and (9), we have the conventional Eulerian description, and if $\hat{u}'_i = \dot{u}_i$, we have the Lagrangean description. With this definition of the material derivative, the incompressible Navier-Stokes equations in the ALE formulation reduce to:

$$\rho \frac{\partial u_i}{\partial t} + \rho c_j \frac{\partial u_i}{\partial x_j} = \frac{\partial \tau_{ij}}{\partial x_j} + b_i \quad (10)$$

2.3. Finite Element Discretization

A finite discretization in primitive variables with fractional time steps (Sampaio, 1993) is used to solve Eq. (10). We use a mixed Petrov-Galerkin formulation, where the momentum equations are first discretized in time with a Crank-Nicholson scheme which is second order accurate. Then a least squares discrete discretization is applied to the spatial domain, in which the squared residual is minimized with respect to velocity components. After a somewhat tedious algebraic manipulation, the final form of the algebraic momentum equations is given by:

$$\begin{aligned}
\int_{\Omega} \frac{\rho}{\Delta t} (W_I) \left(\hat{u}_i^{n+1} + \frac{\Delta t}{2} \hat{u}_j^n \frac{\partial \hat{u}_i^{n+1}}{\partial x_j} \right) d\Omega &= \int_{\Omega} \frac{\rho}{\Delta t} (W_I) \left(\hat{u}_i^n + \frac{\Delta t}{2} \hat{u}_j^n \frac{\partial \hat{u}_i^n}{\partial x_j} \right) d\Omega + \int_{\Omega} \frac{\partial N_I}{\partial x_i} \hat{p}^{n+1/2} d\Omega \\
&- \int_{\Omega} \frac{\Delta t}{2} \hat{c}_k^n \frac{\partial N_I}{\partial x_k} \frac{\partial \hat{p}^{n+1/2}}{\partial x_i} d\Omega - \int_{\Omega} \frac{\partial N_I}{\partial x_j} \mu \left(\frac{\partial \hat{u}_i^n}{\partial x_j} + \frac{\partial \hat{u}_j^n}{\partial x_i} \right) d\Omega + \int_{\Gamma_i} N_I \bar{t} d\Gamma
\end{aligned} \quad (11)$$

where W_I is a Petrov-Galerkin weighting function given by

$$W_I = \left(N_I + \frac{\Delta t}{2} \hat{c}_k^n \frac{\partial N_I}{\partial x_k} \right) \quad (12)$$

The pressure-continuity discrete equation is obtained through the combination of the continuity equation and the minimisation of the momentum equation with respect to the pressure. The resultant approximate weak form is a Poisson-like equation given by

$$\int_{\Omega} \Delta t \frac{\partial N_I}{\partial x_i} \frac{\partial \hat{p}^{n+1/2}}{\partial x_i} d\Omega = - \int_{\Omega} \Delta t \frac{\partial N_I}{\partial x_i} \rho \hat{c}_j^n \frac{\partial \hat{u}_i^n}{\partial x_j} d\Omega - \int_{\Gamma} N_I (\bar{G}^{n+1} - \bar{G}^n) d\Gamma - \int_{\Omega} \rho N_I \frac{\partial \hat{u}_j^n}{\partial x_j} d\Omega \quad (13)$$

It is important to note that in equation (13), the boundary integral is not null only at boundaries with prescribed velocity Γ_U , being different from zero just for moving boundaries Γ_C , i.e.

$$\int_{\Gamma} N_I (\bar{G}^{n+1} - \bar{G}^n) d\Gamma = \int_{\Gamma_U} N_I (\rho u_i^{n+1} n_i^{n+1} - \rho u_i^n n_i^n) d\Gamma = \int_{\Gamma_C} N_I (\rho w_i^{n+1} n_i^{n+1} - \rho w_i^n n_i^n) d\Gamma \quad (14)$$

In the above equations, the superscripts refer to the time steps, Δt is the time step increment, c is the convective velocity, N_I is the finite element shape function for node I , u is the fluid velocity, n_i is the outward pointing unit normal vector, $G = \rho u_i n_i$ is the mass flux, and the remaining variables are as defined before. These equations are solved in a segregated manner, using a preconditioned conjugate gradient method. See Sampaio et al.(1993) for further information.

2.4. Structural Dynamics

In this work we only consider dynamics of rigid bodies. The movement of the body is obtained with a straightforward application of Newmark's method (Hughes, 1987):

$$\mathbf{M} \mathbf{a}^{t+\Delta t} + \mathbf{C} \mathbf{v}^{t+\Delta t} + \mathbf{K} \mathbf{d}^{t+\Delta t} = \mathbf{F}^{t+\Delta t} \quad (15)$$

$$\mathbf{v}^{t+\Delta t} = \mathbf{v}^t + \left[(1-\gamma) \mathbf{a}^t + \gamma \mathbf{a}^{t+\Delta t} \right] \Delta t \quad (16)$$

$$\mathbf{d}^{t+\Delta t} = \mathbf{d}^t + \mathbf{v}^t \Delta t + \left[\left(\frac{1}{2} - \beta \right) \mathbf{a}^t + \beta \mathbf{a}^{t+\Delta t} \right] \Delta t^2 \quad (17)$$

where \mathbf{d} , \mathbf{v} , and \mathbf{a} are the displacements, velocity and acceleration of the body, and β and γ are parameters of the method, and \mathbf{M} , \mathbf{C} , and \mathbf{K} are the mass, damping and stiffness matrices of the structure. In this work we used $\gamma = 1/2$ and $\beta = 1/4$, which leads to an implicit, second order accurate and unconditionally stable time integration scheme. The stability of this scheme is important because the time step increment for the structural time evolution is taken as the same as the time increment chosen for the CFD solution. This time increment is determined by the stability requirements of the CFD algorithm, and therefore its time scale is completely unrelated to the dynamic behavior of the structure.

2.5. Fluid Structural Coupling

The coupling between the fluid and structural field was imposed in a segregated manner, and compatibility conditions are imposed a posteriori, at the end of each time step, to enforce the consistency of the interface between both fields. This approach has the advantage, in contrast to a monolithic approach, that the most efficient numerical solution technique can be used for each particular field.

At the start of each time step, we assume that the interfaces are consistent, i.e., that points lying on the interface between the structural and fluid domain have the same velocities, when considered belonging to either domain. Each domain is then advanced in time independently, according to its own physics. The other domain is considered static, and used only as a source of initial and boundary conditions for the current time step. At the end of the time step, the interfaces will therefore no longer be consistent, so in fact a series of predictor-corrector steps is repeated until satisfactory agreement between the two fields is reached. As the interfaces between domains move along the time, the mesh is distorted by the movement of the boundaries of the domain, and when this distortion becomes excessive, the inadequate elements are removed and the mesh is recreated in these regions. The predictor-corrector technique adopted is adapted from the one proposed by Bloom et al. (1998), and the general procedure is summarized below:

- a. *For all time step do:*
- b. *Estimate a predictor velocity V_p*
- c. *Move structure and mesh in the computational domain*
- d. *If the quality of the mesh is not satisfactory, then:*
- e. *Delete distorted elements and recreate mesh*
- f. *Interpolate solution to the new mesh*
- g. *Solve the CFD problem*
- h. *Solve the structural dynamics problem*
- i. *Compute a corrector velocity V_c*
- j. *If V_p and V_c converged to each other, then:*
- k. *Advance to next time step*
- l. *Else:*
- m. *$V_p = V_c$*
- n. *Repeat from step c*

The predictor velocity V_p at the start of each time increment (step b) is taken as an estimate of the current velocity of the structure. This velocity is computed by a simple linear extrapolation from the structural velocity and acceleration computed at the previous time step. As the interpolation of solutions between meshes (step f) is not cheap and can introduce errors, we try to minimize it by restricting the regions where the mesh is allowed to move. This will be described further below. The CFD solution (step g) uses as boundary conditions for the moving boundaries the current velocity of the interface, V_p . The corrector velocity V_c (step i) is the interface velocity that results from the solution of the structural dynamics problem (step h). The convergence test (step j) verifies if the difference between the corrector velocity V_c and V_p are less than some prescribed tolerance. If this is so, the algorithm advances to the next time step (step k), otherwise the current corrector velocity is taken as the new predictor velocity and the predictor-corrector loop is repeated. In this work we only dealt with rigid bodies, therefore the velocity of the interface nodes can be easily computed from the velocity of body with simple transformation matrices (Nomura and Hughes, 1992).

3. Numerical Tools

There are many practical aspects to a successful computational implementation of the procedures described above. Clearly, facilities for dealing with deformable domains, which involve automatic mesh generation, assessment of mesh quality, automatic mesh movement and regeneration are all important aspects. The most interesting aspects of our implementation will be described below.

3.1. Subdomain partitioning

The partition of a domain into simpler subdomains is a well proven practical technique that helps the mesh generation in domains with complex geometry. In this work, this idea is extended and different numerical formulations can be employed for the discretization on each subdomain. We have implemented three distinct possibilities: a conventional Eulerian formulation, an ALE formulation with a deformable mesh and an ALE formulation where the mesh is movable but not deformable. The Eulerian formulation is more appropriate for regions of fluid away from the moving boundaries. The ALE formulation with non-deformable but moving meshes is used in the regions very close to the moving interfaces. These meshes are attached to the moving bodies, and are not deformable because, in general, complex flow phenomena that require very fine and high quality meshes, such as boundary layer formation or separation bubbles, occur in these regions. Deformation of the mesh would quickly destroy the quality of these meshes and compromise the quality of the solution. The ALE formulation with deformable meshes is used to couple the two kinds of domains just described. A simple sketch example can be seen in Fig. (1). For the structure, of course, we use a Lagrangian description.

The use of different formulations for different subdomains is important because it minimizes the needed interpolation of solutions between different meshes. Clearly, in the subdomains where an Eulerian formulation is used, the interpolation is completely unnecessary because the mesh never varies. Interpolation between unstructured meshes, even with the use of adequate data structures to speed up searches, is a somewhat costly procedure. The interpolation can also reduce the accuracy of the numerical solution, therefore it is important that it be restricted to the as small a region as possible. In the current implementation, the subdomain decomposition and the assignment of formulations is done a

priori by the user, therefore some knowledge of the expected amplitudes of displacement is necessary. In practice, however, this has not proven itself to be a problem.

The mesh generation inside each subdomain is fully automatic, using an advancing front mesh generator (Carvalho, 2001). The mesh density is controlled by a background mesh, and of course the generator enforces compatibility between the boundaries of the subdomains. This generator has been modified to produce highly elongated elements along solid surfaces using an advancing layers technique.

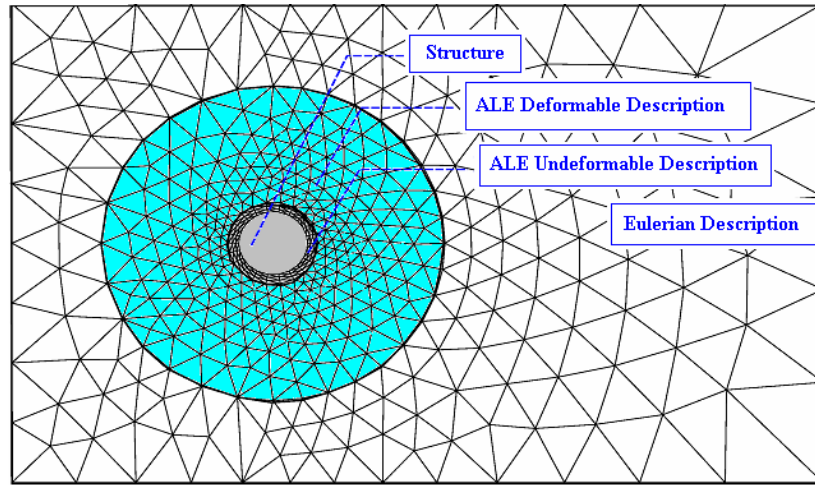


Figure 1. Computational model: subdomain decomposition and different descriptions.

3.2. Mesh Movement and Remeshing

In the domains with a deformable ALE formulation, the movement of the interface nodes causes distortions of the original shapes of the elements connected to these nodes. Two techniques are used to minimize these effects. Initially, a procedure akin to a mesh smoothing is used. The mesh is viewed as a network of elastic springs, where each edge of the mesh corresponds to a spring whose stiffness is inversely proportional to the edge length. Then an elastic problem is solved, where the boundary conditions are given by the new positions of the nodes of the interfaces of the subdomains. A simple direct iteration is done, and typically, very few iterations are sufficient for convergence to the required tolerance. This procedure is therefore very fast. Other alternative that uses a function of the distance to the solid body is also implemented and more details on both options can be seen in Antunes (2002).

There are cases, however, where the distortion of the elements is too severe, and the smoothing procedure breaks down. There are particular configurations, for instance, that are prone to element collapse. When this happens, either the whole mesh is re-generated (global remeshing) or the compromised elements are removed from the mesh and the mesh is re-generated in the remaining “holes” (local remeshing). The same mesh generation algorithm that was used to create the original mesh is used inside each “hole”. This strategy allows for less mesh reconstructions being computationally more efficient. An example of this procedure is shown in Fig. (2).

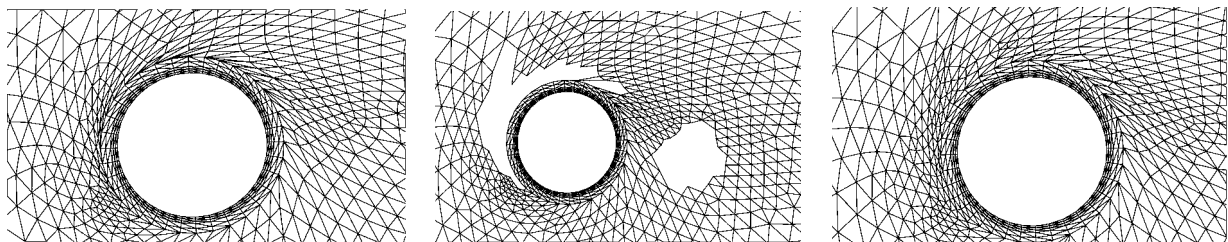


Figure 2. Local remeshing sequence.

4. Applications

The scheme previously described has already been utilized for the simulation of a variety of applications (Antunes et al., 2002, Lyra and Antunes, 2002 and Antunes, 2002), involving different levels of interaction between an external fluid flow and a rigid circular cylinder, including the study of: the flow around a fixed cylinder, the flow around a cylinder with an imposed periodic displacement, the free vibration of the cylinder in a stationary fluid and the coupled fluid-structure problem of a rigid cylinder supported by elastic springs free to interact with the surrounding fluid flow.

In the literature (Hiejima et al., 1997 and references there in) several experimental and numerical results are reported in which acoustic excitation is applied to an external flow to increase the momentum transfer from the outside flow to the boundary layer and so eliminating (or delaying) separation or suppressing (or reducing) vortex induced vibrations in different solid configurations. In this article, our computational system is used to perform an initial study on the behavior of the fluid-structure problem described by Hiejima et al. (1997), in which an idealization of the acoustic excitation is obtained through the application of a periodic excitation velocity on two points at the cylinder surface (see Fig. (3)). The angle between the stagnation point and the excitation point is $\phi_a = 80^\circ$. The excitation velocity is given by

$$V_a = U_a \sin(2\pi f_a t) \quad (18)$$

where, U_a and f_a refers to the periodic excitation amplitude and frequency, respectively. The amplitude U_a is chosen to be equal to 10% of the freestream velocity U , and the two excitation velocities are in phase.

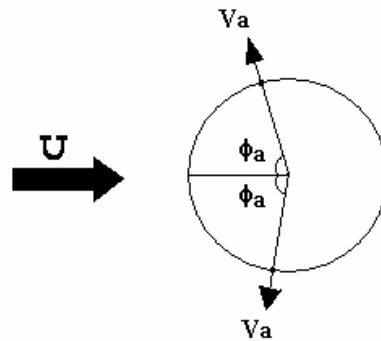


Figure 3. Description of the periodic velocity excitation on the surface of the cylinder.

Figure (4) shows the full description of the numerical model, including the: computational domain, boundary conditions, fluid properties and structural parameters of the solid-spring system. The free stream velocity is $U = 0.0264$ m/s and the Reynolds number based on the cylinder diameter is 2000. Initially we performed some numerical simulations considering a fixed cylinder and the vortex shedding frequency obtained at $Re = 2000$ was $f_s = 0.69$ Hz. This value is higher than that reported by Hiejima et al. (1997), equal to 0.55Hz, but still in good agreement with the experimental curve presented by Blevins, 1986. The cylinder-spring parameters adopted here are that adopted by Hiejima et al. (1997), except the mass which are determined so that the natural frequency of the system is equal to the vortex shedding frequency of 0.69Hz. Therefore, for the values we obtained for the vortex shedding frequency ($f_s = 0.69$ Hz), this thus corresponds to the resonance frequency. These differences from the Hiejima et al. (1997) values have to be taken into account when comparing our results with theirs.

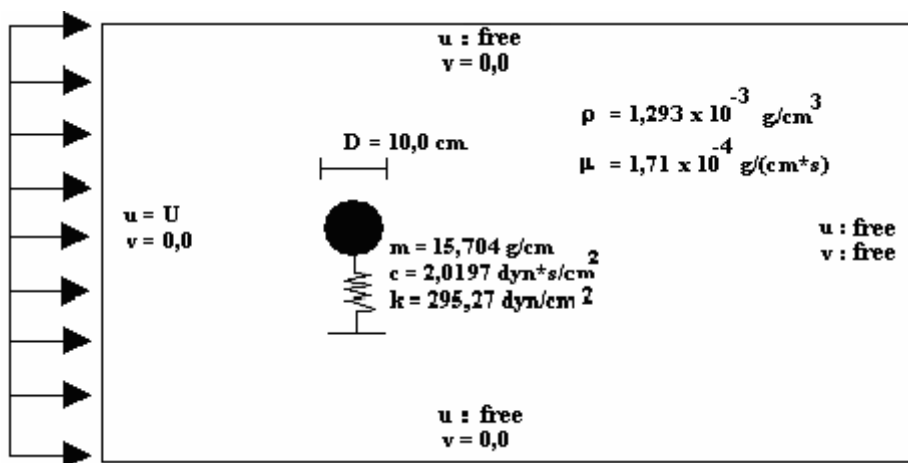


Figure 4. Computational model: data and boundary conditions.

The domain was subdivided in subdomains where the different descriptions are utilized in order to facilitate the treatment of problems involving multiple physics as shown in Fig. (1). The finite element mesh adopted consists of a triangularization with 12076 elements and 6122 nodes. The circular cylinder is centred on the origem of the coordinates axes, and the portion of the ALE mesh is restricted to the circular region around the cylinder with diameter 1 m. The domain consists in a rectangle whose coordinates in meters are: $(-0.65; -0.65)$, $(1.80; -0.65)$, $(1.80; 0.65)$ e $(-0.65; 0.65)$.

The effect of the periodic velocity excitation was investigated considering different ratio between the values of the excitation frequency (f_a) and the vortex shedding frequency (f_s), i.e. $f_a/f_s = 3.78$; 4.45 and 5.12. Accordingly to Hiejima et al. (1997), the value 4.45 is close to the experimental value near the transition wave frequency, which is an effective value of frequency for an acoustic excitation to change the flow around a stationary circular cylinder. With such value of excitation they were able to get a considerable increase on the vortex shedding frequency that was quite effective in reducing the vortex induced vibration amplitude, as the experimental results suggests. We picked up two other values around 4.45 in order to study the influence of the excitation frequency on our results.

Considering a fixed cylinder and the different ratio mentioned previously, the frequency of the velocity transversal to the flow in a point located inside the vortex shedding was studied. The frequency of the transversal velocity with and without the periodic excitation are plotted in Fig. (5). It can be observed that the periodic excitation modify this frequency and so the vortex shedding frequency.

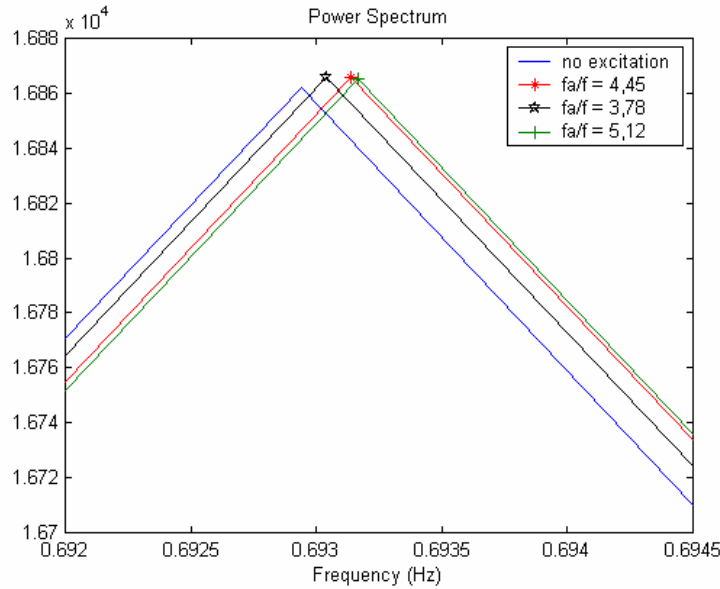


Figure 5. Frequency spectrum of the transversal velocity.

The same analysis were performed considering the cylinder free to vibrate on the direction transversal to the flow. The numerical simulation set up consists on starting with a fixed cylinder and after the vortex shedding became periodic we allow the transversal movement and after the vibration amplitude stabilizes on a constant value we start applying the periodic excitation. In all three cases the cylinder is set free after 25000 time steps and the excitation starts after 50000 time steps. In figure (6), (7) and (8) the displacement histories are plotted for $f_a/f_s = 3.78$; 4.45 and 5.12, respectively. In Fig. (6), $f_a/f_s = 3.78$, there is no reduction but a small increase on the oscillatory amplitude, and the adopted excitation frequency has an adverse effect. In Fig. (7), with $f_a/f_s = 4.45$, the transversal displacement amplitude reduces and we notice the presence of the pulse phenomena. For $f_a/f_s = 5.12$, Fig. (8), we have the most effective (for the three values analysed) reduction on the amplitude of the oscillation. The modification on amplitudes occurs due to the modification on the vortex shedding frequency and the biggest reduction on the amplitude corresponds to the biggest increase on the vortex shedding frequency as can be seen in Fig. 5.

For $f_a/f_s = 4.45$ and 5.12 the vortex shedding frequency differs more from the cylinder natural frequency (or resonance frequency) than for $f_a/f_s = 3.78$ and the results suggest that an even bigger variation on the vortex shedding frequency can reduce mode or even suppress the vibration on the cylinder.

It should be observed that the amplitude of the oscillations were small with the cylinder vibrating under the influence of the vortex formation and shedding behind the cylinder, and that the characteristic of the vortex induced vibrations were directly affected by the change on the frequency of such vortex formation and shedding. Qualitatively we were able to reproduce the expected results, but further investigation on the disagreement on the vortex shedding frequency for the fixed cylinder must be pursued. Also, further investigation considering different ration between the values of the excitation frequency (f_a) and the vortex shedding value (f_s), and also considering different application points and amplitude of excitation must be pursued in order to get a better insight on the behaviour of such application.

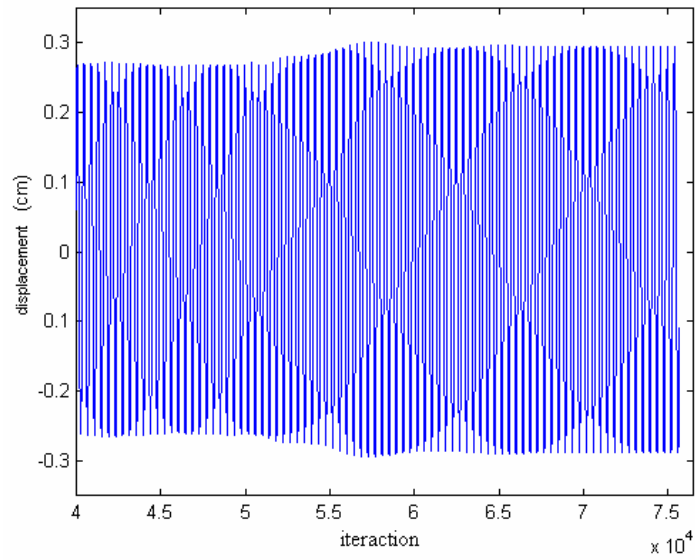


Figure 6. Time history of transversal displacement for $f_a / f_s = 3.78$.

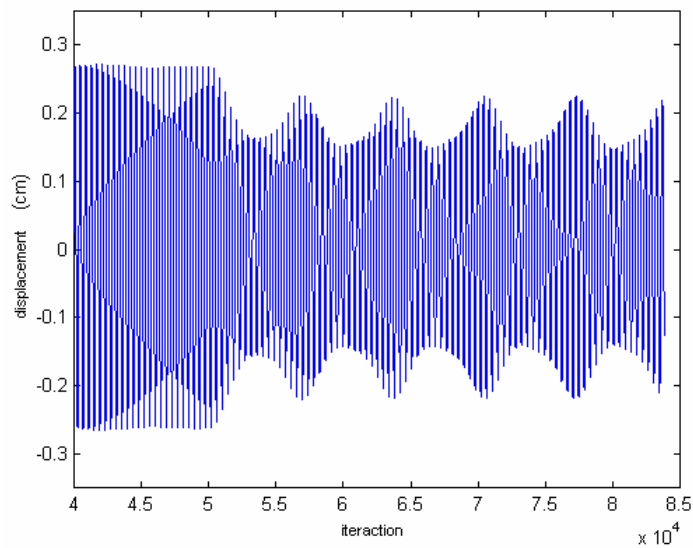


Figure 7. Time history of transversal displacement for $f_a / f_s = 4.45$.

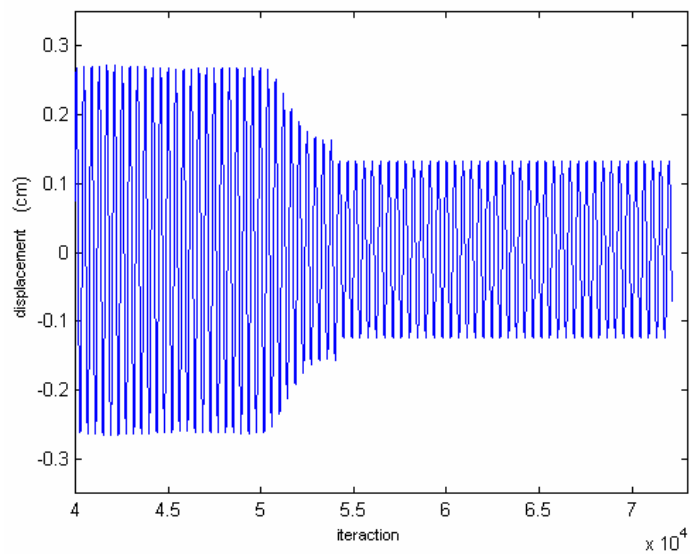


Figure 8. Time history of transversal displacement for $f_a / f_s = 5.12$.

4. Conclusions

A brief description of the developed computational system for fluid-structure interaction analysis was presented. Such system incorporates several important tools (different mesh movement algorithms; possibility to decompose the domain into several subdomains with different reference frame description and to use global or local adaptive remeshing strategies) which renders it very flexible and capable to deal with a large class of two dimensional applications. Some of these tools and strategies were not exploited in this application and must also be tested with more complex problems to stress their real importance. The results obtained through the study of using periodic “acoustic” excitation to suppress the vortex induced vibration on a circular cylinder are qualitatively consistent with the literature, however they are just preliminary and requires further investigation. The fluid dynamics solver using the adopted formulation has severe limitation in terms of the time step size leading to a large number of iterations and improvements on this feature or an alternative formulation without so strong constrain must be investigated. Finally, other improvements are required in terms of efficiency to allow the analysis of large-scale problems within an acceptable time. This improvements would involve, for instance, the incorporation of an error estimator to control the adaptive procedure, a parallel or parallel/vector implementation and others elements of high performance computation. Some of this aspects are already under investigation.

5. Acknowledgement

The authors would like to thank the Brazilian Government, through the Agencies CAPES, CNPq and MCT-ANP for the financial support provided.

6. References

- Antunes, A. R. E., 2002, “A Flexible Computational System Using an “ALE” Finite Element Formulation for the Analysis of Fluid-Structure Interaction Problems”. Master dissertation, Mechanical Engineering Department, Federal University of Pernambuco (UFPE), Recife/PE, Brasil, 83 p. (in Portuguese).
- Antunes, A. R. E., Carvalho, D. K. E., and Lyra, P. R. M., 2002, “Different Strategies for Mesh Movement and Remeshing of Unstructured Meshes Used When Dealing with Fluid-Structure Interaction Problem”, 9th Brazilian Congress of Thermal Engineering and Science, Caxambu, Brasil (in Portuguese and in CD-ROM).
- Blevins, R. D., 1986, “Flow-Induced Vibration”, R. E. Krieger Publishing, Inc, Malabar/Florida, USA, 363 p.
- Blom, J. F. and Leyland, P., 1998, “Consistency Analysis of Fluid-Structure Interaction Algorithms”, European Cong. on Comp. Methods in App. Science and Eng. (ECCOMAS), Barcelona, Spain, 15 p. (in CD-ROM).
- Brooks, A. N. and Hughes, T. J. R., 1982, “Streamline Upwind/Petrov-Galerkin Formulations for Convection Dominated Flows with Particular Emphasis on the Incompressible Navier-Stokes Equations”, Computer Methods in Applied Mechanics and Engineering, Vol. 32, pp. 199-259.
- Carvalho, D. K. E., 2001, “A Computational System for Two dimensional Unstructured Mesh Generation and Adaptation”. Master dissertation, Mechanical Engineering Department, Federal University of Pernambuco (UFPE), Recife/PE, Brasil, 70 p. (in Portuguese).
- Childs, S. J., 1999, “The Energetic Implications of Using Deforming Reference Descriptions to Simulate the Motion of Incompressible Newtonian Fluids”, Computer Methods in Applied Mechanics and Eng., vol. 180, pp 219-238.
- Hiejima, S., Nomura, T., Kimura, K. & Fujino, Y., 1997, “Numerical Study on the Suppression of the Vortex-Induced Vibration of a Circular Cylinder by Acoustic Excitation”, Journal of Wind Engineering and Industrial Aerodynamics, vol. 67 & 68, pp 325-335.
- Hughes, T.J.R., Liu, W.K. and Zimmermann, T.K., 1981, “Lagrangian-Eulerian Formulation for Incompressible Viscous Flows”, Computer Methods in Applied Mechanics and Engineering, vol. 29, pp. 329-349.
- Hughes, T. J. R., 1987, “The Finite Element Method”, 1st Edition, United States of America, Prentice-Hall, Inc., 803p.
- Lyra, P.R.M. and Antunes A. R. E., 2002, “The Analysis of Fluid-Structure Interaction Using an ALE Finite Element Formulation”, Third Joint Conference of Italian Group of Computational Mechanics (GIMC 2002) and Iberian Latin American Cong. on Comp. Meth. in Eng. (CILAMCE 2002), Giulianova-Teramo, Italy, 10p. (in CD-ROM).
- Nomura, T. and Hughes, T.J.R., 1992, “An Arbitrary Lagrangian-Eulerian Finite Element Method for Interaction of Fluid and a Rigid Body”, Computer Methods in Applied Mechanics and Engineering, vol. 95, pp. 115-138.
- Sampaio, P. A. B., Lyra, P. R. M., Morgan and K., Weatherill, N., 1993, “Petrov-Galerkin Solutions of Incompressible Navier-Stokes Equations in Primitive Variables with Adaptive Remeshing”, Computer Methods and Applied Mechanics and Engineering, vol. 106, pp. 143-178.